

Supporting Information

Distinct structure assembly driven by metal-ligand binding in Au₂₃ nanoclusters and its relation to photocatalysis

Shuohao Li,^a Yongnan Sun,^a Chenyang Wu,^a Weigang Hu,^a Wei Li,^a Xu Liu,^a Mingyang Chen,^b and Yan Zhu^{*a}

^aSchool of Chemistry and Chemical Engineering, Nanjing University, Nanjing 210093, China

^bCenter for Green Innovation, School of Materials Science and Engineering, University of Science and Technology Beijing, Beijing 100083, China

Experimental Section

Synthesis of Au₂₃(SR)₄(PPh₃)₉ (SR = 2-mercaptobenzoxazole)

The Au(PPh₃)Cl (0.162 mmol) was dissolved in 6 mL ethanol with stirring for about 30 min. Then, the NaBH₄ (0.338 mmol) was dissolved in 2 mL ethanol and quickly added into the mixed solution. After stirring for 10 min, the mixed solution was evaporated and dissolved in 10 mL acetone with 2-mercaptobenzoxazole (0.132 mmol). The mixed solution was heated to 70 °C and maintained at this temperature. After stirring for 1 h, the mixed solution was evaporated and washed with ethyl ether for 2-3 times. The crude product was dissolved in CH₂Cl₂, and then separated and purified by PTLC. The single crystal was acquired by vapor diffusion of n-hexane into a DCM solution over one week at room temperature. A crystal of Au₂₃(SR)₄(PPh₃)₉ suitable for single-crystal X-ray analysis was collected directly from the mother liquor.

Synthesis of Au₂₃(SR')₁₆ (SR' = Cyclohexanethiol)

HAuCl₄·3H₂O (0.3 mmol) and tetraoctylammonium bromide (TOAB, 0.348 mmol) were dissolved in 12 mL CH₃OH. 1-cyclohexanethiol (1.6 mmol) was added to the mixture after stirring for 15 min. After 2 h, NaBH₄ (3 mmol dissolved in 6 mL of cold water) was quickly added to the solution under vigorous stirring. After one day, the

reaction mixture was precipitated out of the CH₃OH and the Au₂₃(SR')₁₆ clusters was obtained.^{S1}

Au clusters supported on TiO₂ or SiO₂

The 2 mg Au₂₃(SR)₄(PPh₃)₉ or Au₂₃(SR')₁₆ cluster and 100 mg TiO₂ (TiO₂ was purchased from Shanghai Macklin Biochemical Co., Ltd) were adequately mixed via solid phase grinding for 20 min, which was used for photocatalytic degradation of rhodamine B and methyl orange. In addition, the 6 mg Au₂₃(SR)₄(PPh₃)₉ or Au₂₃(SR')₁₆ cluster 60 mg commercial SiO₂ were adequately mixed via solid phase grinding for 20 min, which was used for photocatalytic degradation of tetracycline.

Photocatalytic performance test

The 40 mg Au₂₃(SR)₄(PPh₃)₉/TiO₂ or Au₂₃(SR')₁₆/TiO₂ catalysts and 20 mL rhodamine B or methyl orange (C₀ = 5 ppm) were separately transferred to a heat-resistant glass photocatalytic reactor. A circulating water system was used to maintain the reaction temperature at room temperature. Firstly, they were magnetically agitated for 30 min in the dark to achieve an adsorption-desorption equilibrium of the dye and catalyst. The reaction was performed as a light source with a 300 W Xe lamp 400 nm cut-off filter. The rhodamine B or methyl orange concentration was measured using an ultraviolet-visible spectrophotometer (Shimadzu, UV-1800), and the initial concentration (C₀) was determined by the concentration after reaching adsorption equilibrium in the dark.

In addition, the prepared 30 mg Au₂₃(SR)₄(PPh₃)₉/SiO₂ or Au₂₃(SR')₁₆/SiO₂ catalysts and 20 mL tetracycline (C₀ = 20 ppm) were separately transferred to a heat-resistant glass photocatalytic reactor with a 300 W Xe lamp without filter. Other experimental operation was consistent with the above.

Characterization.

The X-ray crystallography was performed on a Bruker D8 VENTURE with Mo K α radiation ($\lambda = 0.71073 \text{ \AA}$). ESI mass spectra were recorded on a Waters QT of mass spectrometer using a Z-spray source. The clusters were first dissolved in CH₂Cl₂ (~0.5 mg/ml) and directly infused into the chamber at 5 μ L/min. The source temperature was kept at 70 °C, the spray voltage was 2.20 kV, and the cone voltage was adjusted to 60 V. Optical absorption spectra were recorded on a UV-vis spectrometer using SHIMADZU UV-1800. The binding energies of the catalysts were determined by X-ray photoelectron spectroscopy (XPS) (Thermo Scientific K-Alpha) using Al K α ($h\nu =$

1486.6 eV) as the excitation source. Correction of the charge effect was made with the C (1s) peak at 284.6 eV. The Electron paramagnetic resonance (EPR) spectra were conducted on a Bruker 500 spectrometer at room temperature. The low-temperature EPR experiment was performed at 2 K, and conducted on a Bruker EMX plus 10/12 (equipped with Oxford ESR910 Liquid Helium cryostat). A home-built wide-field fluorescence microscope based on Olympus IX73 was used with 450 nm CW diode laser for the PL lifetime measurement, which was done by using a single photon counting system (TCSPC, PicoHarp 300). The photoelectrochemical (PEC) and electrochemical impedance spectroscopy (EIS) measurement were performed on a CHI660B electrochemical workstation in a standard three-electrode system with a platinum foil as a counter electrode, a glassy carbon as working electrode and a saturated Ag/AgCl as a reference electrode. A 300W Xe lamp was utilized as the light source on the measurement, which were carried out at room temperature in 1 mol/L Na₂SO₄. The measurement of quantum yield was performed as a light source with a 300 W Xe lamp under monochromatic light of different wavelengths (420, 520, 600 and 700 nm respectively). Apparent quantum efficiency (AQE) was defined as the following equation ^{S2}.

$$\Phi_{AQY} (\%) = \frac{[\text{Rhodamine B degraded (mol)}] \times 2}{\text{photon number entered the reaction vessel (mol)}} \times 100$$

Computational Details

The structures of single-unit Au₂₃(SR)₄(PPh₃)₉ and Au₂₃(SR')₁₆ were extracted from the crystal structures and then optimized using the full atomistic structural models at the density functional (DFT) level with the PBE^{S3} functional and the LANL2DZ^{S4} basis set and pseudopotential. The partial density of states (PDOS) of the two clusters were evaluated for the fully optimized geometries at PBE/LANL2DZ level. All of the calculations were performed with Gaussian09^{S5} suite of software.

Supporting Figures

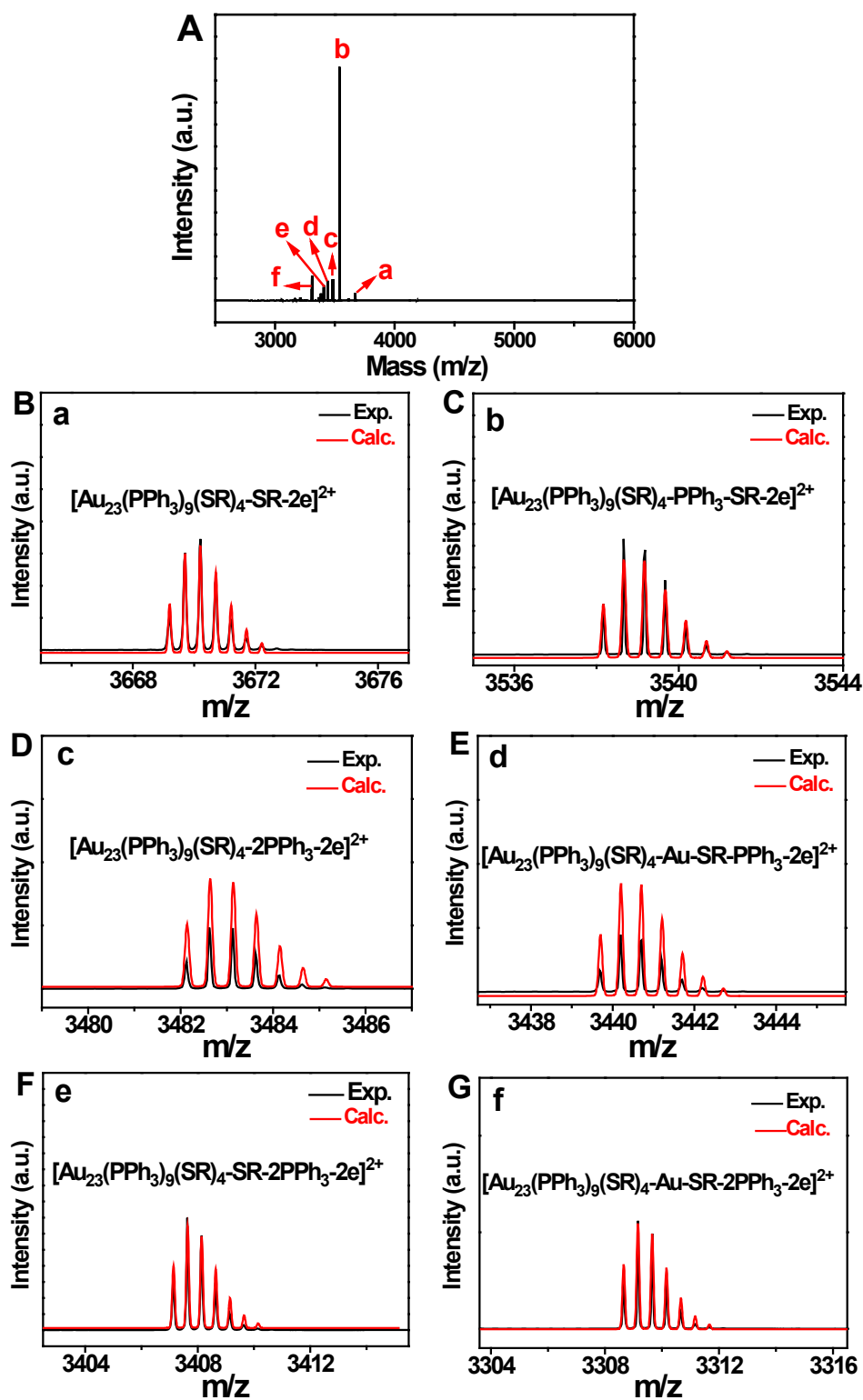


Fig. S1. (A) ESI-MS spectrum of the $\text{Au}_{23}(\text{SR})_4(\text{PPh}_3)_9$ cluster (where $\text{SR} = \text{C}_7\text{H}_4\text{NOS}$). (B-G) Comparison of the experiment (black) and simulated (red) isotopic patterns, which respectively correspond to the peaks of a, b, c, d, e and f in A.

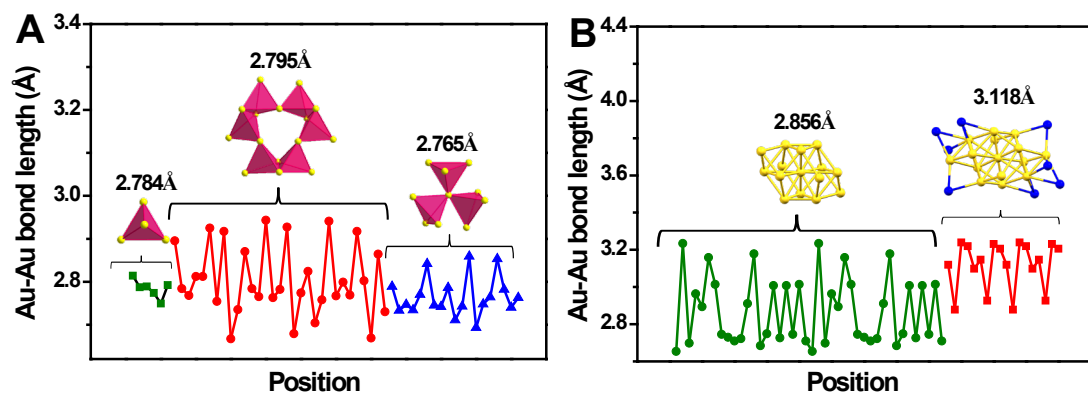


Fig. S2. Distribution of Au-Au bond lengths from the different positions of the Au atoms of (A) $\text{Au}_{23}(\text{SR})_4(\text{PPh}_3)_9$ and (B) $\text{Au}_{23}(\text{SR}')_{16}$.

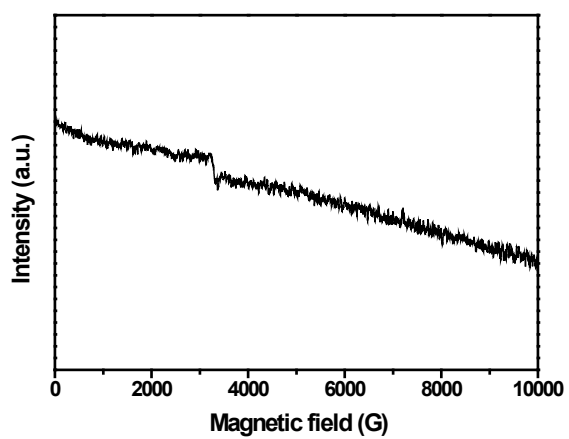


Fig. S3. The EPR spectrum of the $\text{Au}_{23}(\text{SR})_4(\text{PPh}_3)_9$ clusters recorded at 2 K.

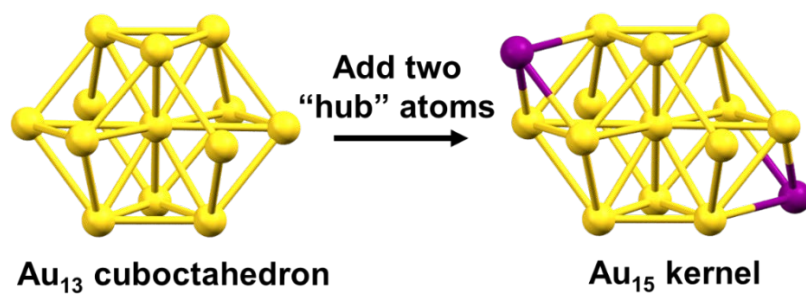


Fig. S4. The Au_{15} kernel by adding the two "hub" Au atoms onto the Au_{13} cuboctahedron toward $\text{Au}_{23}(\text{SR})_{16}$ cluster.

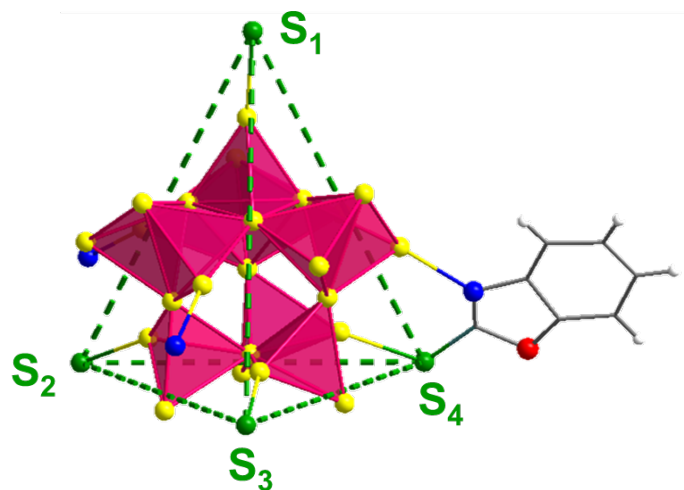


Fig. S5. The S atoms of four C_7H_4NOS ligands constitute a tetrahedral framework and act as a bracket to support the $Au_{23}(SR)_4(PPh_3)_9$ cluster, and phosphine ligands linked to Au atoms omitted for clarity. Color labels: yellow = Au; green = S; blue = O; red = N; gray = C; white = H. Most H atoms are omitted for clarity.

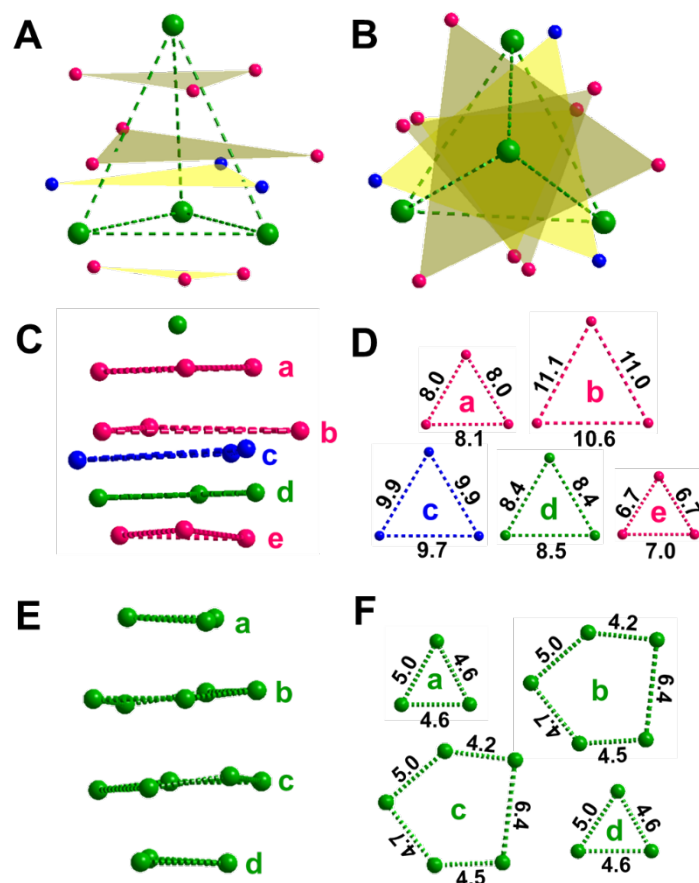


Fig. S6. (A-D) The S, P, O atoms arrangements of the dual ligands on $\text{Au}_{23}(\text{SR})_4(\text{PPh}_3)_9$. (E, F) The S atoms arrangements of the thiolate ligand on $\text{Au}_{23}(\text{SR}')_{16}$. Color labels: green = S; magenta = P; blue = O. The H and C atoms are omitted for clarity

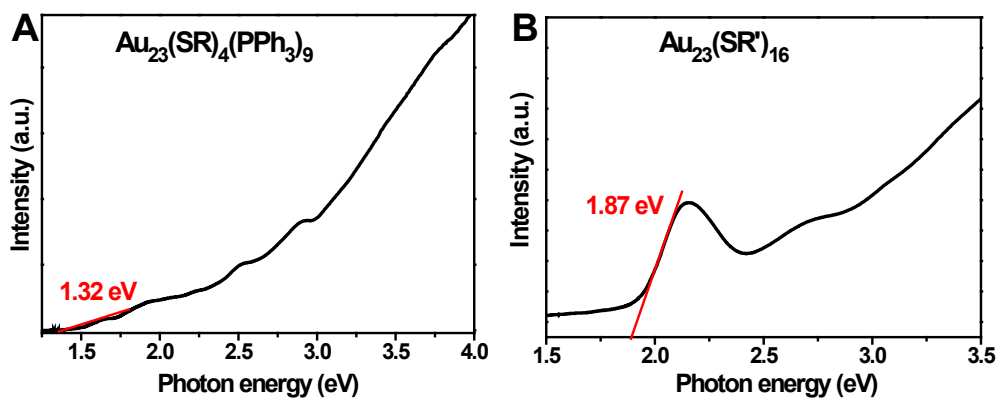


Fig. S7. UV-vis absorption spectra of (A) $\text{Au}_{23}(\text{SR})_4(\text{PPh}_3)_9$ and (B) $\text{Au}_{23}(\text{SR}')_{16}$ on photon energy scale.

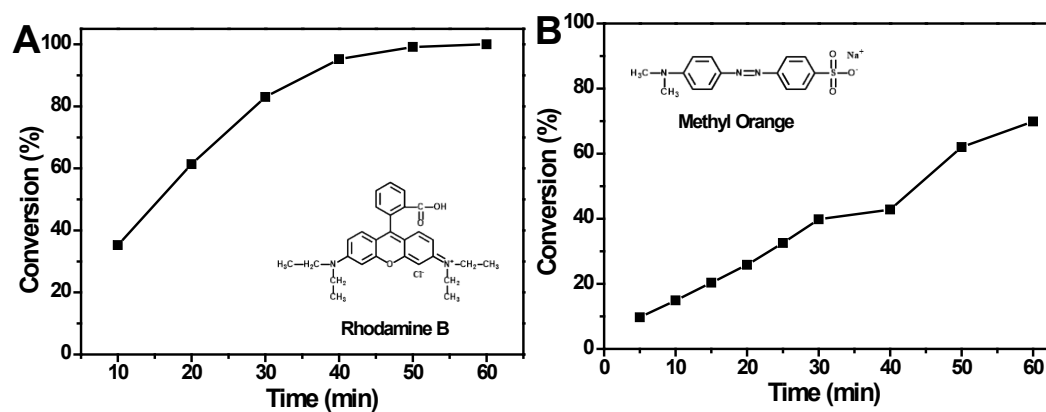


Fig. S8. The photocatalytic performances of TiO₂ for the degradation of (A) rhodamine B and (B) methyl orange under visible-light irradiation (300 W Xe lamp with filter, $\lambda > 400$ nm).

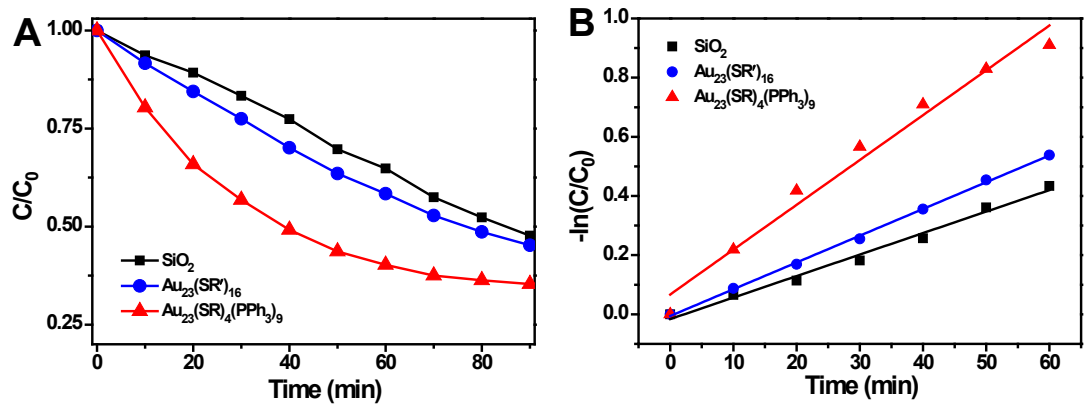


Fig. S9. (A) Photocatalytic activities of different catalysts for the photodegradation of tetracycline (300 W Xe lamp without filter). (B) Kinetic rate constants of tetracycline over different catalysts.

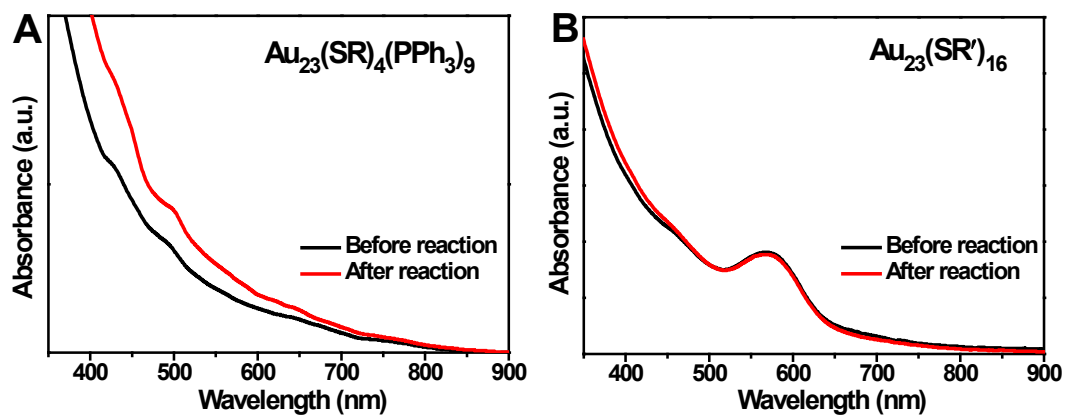


Fig. S10. UV-vis spectra of (A) $\text{Au}_{23}(\text{SR})_4(\text{PPh}_3)_9$ and (B) $\text{Au}_{23}(\text{SR}')_{16}$ before and after photocatalytic reactions.

Table S1. The quantum efficiency of $\text{Au}_{23}(\text{SR})_4(\text{PPh}_3)_9$ and $\text{Au}_{23}(\text{SR}')_{16}$ clusters for rhodamine B under monochromatic light of different wavelengths.

Photocatalysts	Φ_{AQY} (%)			
	420 nm	520 nm	600 nm	700 nm
$\text{Au}_{23}(\text{SR})_4(\text{PPh}_3)_9/\text{TiO}_2$	0.02	0.037	0.012	0.004
$\text{Au}_{23}(\text{SR}')_{16}/\text{TiO}_2$	0.01	0.014	0.004	0.001

Supporting References

- S1 A. Das, T. Li, K. Nobusada, C. Zeng, N. L. Rosi and R. Jin, *J. Am. Chem. Soc.*, 2013, **135**, 18264-18267.
- S2 H. Li, J. Shang, Z. Ai and L. Zhang, *J. Am. Chem. Soc.*, 2015, **137**, 6393-6399.
- S3 J. P. Perdew, K. Burke and M. Ernzerhof, *Phys. Rev. Lett.*, 1996, **77**, 3865-3868.
- S4 P. J. Hay and W. R. Wadt, *J. Chem. Phys.*, 1985, **82**, 270.
- S5 M. J. Frisch, G. W. Trucks, H. B. Schlegel, G. E. Scuseria, M. A. Robb, J. R. Cheeseman, G. Scalmani, V. Barone, B. Mennucci, G. A. Petersson, H. Nakatsuji, M. Caricato, X. Li, H. P. Hratchian, A. F. Izmaylov, J. Bloino, M. Sonnenberg, M. Hada, K. Ehara, R. Toyota, J. Fukuda, M. Hasegawa, T. Ishida, Y. Nakajima, O. Honda, H. Kitao, T. Nakai, J. Vreven, A. J. Montgomery, J. E. Peralta, F. Ogliaro, M. Bearpark, J. J. Heyd, E. Brothers, K. N. Kudin, V. N. Staroverov, T. Keith, R. Kobayashi, J. Normand, K. Raghavachari, A. Rendell, J. C. Burant, S. S. Iyengar, J. Tomasi, M. Cossi, N. Rega, J. M. Millam, M. Klene, J. E. J. Knox, B. Cross, V. Bakken, C. Adamo, J. Jaramillo, R. Gomperts, R. E. Stratmann, O. Yazyev, A. J. Austin, R. Cammi, C. Pomelli, J. W. Ochterski, R. L. Martin, K. Morokuma, V. G. Zakrzewski, G. A. Voth, P. Salvador, J. J. Dannenberg, S. Dapprich, A. D. Daniels, O. Farkas, J. B. Foresman, J. V. Ortiz, J. Cioslowski and D. J. Fox, Gaussian, Inc., Wallingford CT, 2009.